

Optimization of lateral resisting system of framed tubes combined with outrigger and belt truss

Mehrdad Mohammadnejad*¹ and Hasan Haji Kazemi^{2a}

¹Department of Civil Engineering, Birjand University of Technology, Birjand, Iran

²Department of Civil Engineering, Faculty of Engineering, Ferdowsi University of Mashhad, Mashhad, Iran

(Received November 25, 2020, Revised October 29, 2021, Accepted November 4, 2021)

Abstract. In this paper, the optimum location of the belt truss-outrigger for a combined system of framed tube, shear core and outrigger-belt truss is calculated. The optimum location is determined by maximization of the first natural frequency. The framed tube is modeled using a non-prismatic cantilever beam with hollow box cross section. The governing differential equation is solved using the weak form integral equations and the natural frequencies of the structure are calculated. The graphs are introduced for quick calculation of the first natural frequency. The location of the belt truss-outrigger that maximizes the first natural frequency of the structure is introduced as an optimum location. The structure is modeled using SAP-2000 finite elements software. In the modelling, the location of the belt truss-outrigger is changed along the height of the structure. With various locations of the outrigger, the lateral deflection of the all stories and axial force in the columns of the outer tube are calculated. The analysis is repeated by locating the outrigger-belt truss at the optimum location. The analysis results are compared and effect of the optimum location on the lateral deflection and the shear lag phenomena are investigated.

Keywords: framed tube; lateral deflection; natural frequency; optimum location; outrigger-belt truss; shear lag

1. Introduction

In recent years, tubular building has been accepted as an economical and developed structural system. The dynamic behaviors of structural systems can be estimated by Eigen frequency which describes structural stiffness. In general, maximizing the first-order Eigen frequency can be an objective for dynamic topology optimization problems since stiffness of structures also increases when Eigen frequency increases (Lee *et al.* 2012, Pedersen 2000). The problem of optimum reinforcement of a structure to alter its response in free vibration has been considered (Diaz and Kikuchi 1992). In this paper, the goal was to increase the fundamental frequency of a two-dimensional structure. Minimum compliance, or maximum stiffness, is a commonly selected objective, which can be used in its own merit and also as a surrogate to explore other metrics, such as buckling and stability, natural frequencies, Eigen modes, second order effects, etc., depending

*Corresponding author, Assistant Professor, E-mail: mohammadnejad@birjandut.ac.ir

^aProfessor, Email: hkazemi@um.ac.ir

on the problem being explored (Beghini 2014). The optimization problem has been formed based on a preselected value for the fundamental natural frequency, and it has been formulated for minimum structural weight (Alavi *et al.* 2018). A dynamic analysis of the combined system of framed tube and shear walls by Galerkin method using B-spline functions has been presented (Rahgozar *et al.* 2015). Analytic analyses have been carried out on the basis of the principle of minimum potential energy (Rahgozar *et al.* 2014, Malekinejad *et al.* 2016). In these papers, a continuous-discrete approach based on the concept of lumped mass and equivalent continuous approach has been proposed. A new and simple solution for determining the natural frequencies of framed tube combined with shear-walls and tube-in-tube systems has been presented (Mohammadnejad and Haji Kazemi 2018). The weak form integral equations have been presented for calculation of the natural frequencies of a combined system of the framed tube, shear core and outrigger-belt truss (Mohammadnejad and Haji Kazemi 2017). The optimal position of outriggers on the base of the structural roof deflection has been obtained (Zhou *et al.* 2016). In this paper, the theoretical method of inter-story drift-based optimal location of outriggers has been presented. The optimum location of the outrigger braced high-rise shear walls has been determined (Hoenderkamp 2008). The seismic behavior of outrigger-braced building considering the soil-structure interaction based on finding the best location of outrigger and belt truss system has been investigated (Tavakoli *et al.* 2019). The effect of blast phenomenon on the best location of belt truss system has been investigated (Tavakoli *et al.* 2018). The optimum location of a flexible outrigger system based on maximizing the outrigger-belt truss system's strain energy has been determined (Kamgar and Rahgozar 2017). The first natural frequency of tall buildings including framed tube, shear core, belt truss and outrigger system with multiple jumped discontinuities in the cross section of framed tube and shear core has been determined (Kamgar and Saadatpour 2012). Many researchers have investigated free vibration of the tall structures and optimization problems using various approaches (Malekinejad and Rahgozar 2013, Akbulut *et al.* 2020, Karimi *et al.* 2020, Gholipour and Mazloom 2018, Tejani *et al.* 2017, Mortazavi and Toğan 2017, Kaveh and Ilchi Ghazaan 2016, Farghaly 2016, Kaviani *et al.* 2008, Lee *et al.* 2008, Hoenderkamp 2003).

2. Formulation and solution

By applying Hamilton principle, the governing differential equation of motion of framed tube is obtained as follows (Malekinejad and Rahgozar 2012):

$$\frac{\partial}{\partial x} [GA(x) \frac{\partial}{\partial x} W(x,t)] - \frac{\partial^2}{\partial x^2} [EI(x) \frac{\partial^2}{\partial x^2} W(x,t)] - m(x) \frac{\partial^2}{\partial t^2} W(x,t) = 0, \quad 0 < x < L \quad (1)$$

In which, $W(x,t)$, L , $m(x)$, $EI(x)$ and $GA(x)$ are lateral deflection of framed tube, height of the structure, the mass per unit length, flexural stiffness and the shear stiffness of the framed tube, respectively. The flexural stiffness $EI(x)$ depends on both modulus of elasticity E and inertia moment of the cross-section $I(x)$. The shear stiffness $GA(x)$ depends on both shear modulus of elasticity G and cross-sectional area $A(x)$. In another research paper (Mohammadnejad and Haji Kazemi 2017), we have used the weak form integral equations approach in order to solve the Eq. (1) and to calculate the natural frequencies of the framed tube. We obtained the following system of linear algebraic equations:

In Eq. (2), R is a given positive integer, which is adopted such that the accuracy of the results

$$\sum_{r=0}^R [F_2(m,r) + F_3(m,r) + F_4(m,r) + F_5(m,r) + G(m,r)] c_r = 0 \quad m = 0, 1, 2, \dots, R \quad (2)$$

are sustained. r and m are positive integers which change between 0 to R to construct the functions $F_2(m,r)$, $F_3(m,r)$, $F_4(m,r)$, $F_5(m,r)$ and $G(m,r)$. c_r is the unknown coefficient corresponding to selected r . The functions $F_2(m,r)$, $F_3(m,r)$, $F_4(m,r)$, $F_5(m,r)$ and $G(m,r)$ are obtained as follows:

$$\left\{ \begin{array}{l} F_2(m,r) = \int_0^1 \int_0^1 f_2(\xi, s) s^r \xi^m ds d\xi \\ F_3(m,r) = \int_0^1 \int_0^1 f_3(\xi, s) s^r \xi^m ds d\xi \\ F_4(m,r) = \int_0^1 \int_0^1 f_4(\xi, s) s^r \xi^m ds d\xi v \\ F_5(m,r) = \int_0^1 \int_0^1 f_5(\xi, s) s^r \xi^m ds d\xi \\ G(m,r) = \int_0^1 \xi^{r+m} EI(\xi) d\xi \end{array} \right. \quad (3)$$

In which:

$$\left\{ \begin{array}{l} f_1(\xi, s) = L^2 GA(s) - L^2 G(\xi - s) A'(s) - EI''(s) + \frac{\omega^2 L^4}{2} (\xi - s)^2 m(s) \\ f_2(\xi, s) = L^2 G(\xi - s) A(s) - \frac{L^2 G}{2} (\xi - s)^2 A'(s) + 2EI'(s) - (\xi - s) EI''(s) + \frac{\omega^2 L^4}{6} (\xi - s)^3 m(s) \\ f_3(\xi, s) = \frac{\xi^2}{2K} M_1(s) - \frac{\omega^2 L^4}{6} \xi^3 m(s) \\ f_4(\xi, s) = \frac{\xi^2}{2K} M_2(s) \\ f_5(\xi, s) = \frac{\xi^2}{2K} M_3(s) \end{array} \right. \quad (4)$$

And

$$\left. \begin{aligned}
 M_1(s) &= \left[\begin{aligned}
 &\omega^2 L^4 (1-s) - \omega^2 L^4 - \frac{\omega^2 L^6 GA(1)}{6EI(1)} - \frac{k_{e_1} L^5 \omega^2 \xi_1^3 I'(\xi_1)}{3EI^2(\xi_1)} - \frac{k_{e_1} L^5 \omega^2 \xi_1^2}{EI(\xi_1)} - \frac{k_{e_2} L^5 \omega^2 \xi_2^3 I'(\xi_2)}{3EI^2(\xi_2)} \\
 &-\frac{k_{e_2} L^5 \omega^2 \xi_2^2}{EI(\xi_2)} \\
 &-L^2 GA'(s) + \frac{L^2 GA(1)}{EI(1)} f_2(1,s)
 \end{aligned} \right]_{m(s)} \\
 M_2(s) &= \frac{2k_{e_1} L}{EI(\xi_1)} f_1(\xi_1, s) + \frac{2k_{e_1} LI'(\xi_1)}{EI^2(\xi_1)} f_2(\xi_1, s) \\
 M_3(s) &= \frac{2k_{e_2} L}{EI(\xi_2)} f_1(\xi_2, s) + \frac{2k_{e_2} LI'(\xi_2)}{EI^2(\xi_2)} f_2(\xi_2, s) \\
 K &= -\frac{L^2 GA(1)}{2EI(1)} - \frac{2K_{e_1} LI'(\xi_1)}{2EI^2(\xi_1)} \xi_1^2 - \frac{2K_{e_1} L \xi_1}{EI(\xi_1)} - \frac{2K_{e_2} LI'(\xi_2)}{2EI^2(\xi_2)} \xi_2^2 - \frac{2K_{e_2} L \xi_2}{EI(\xi_2)}
 \end{aligned} \right\} \quad (5)$$

In this relation, s and ζ are the non-dimensional location parameters ($\zeta = \frac{x}{L}$). The system of linear algebraic equations (2) may be expressed in matrix notations as follows:

$$\left\{ \begin{aligned}
 &[A]_{(R+1) \times (R+1)} [C]_{(R+1) \times 1} = [0]_{(R+1) \times 1} \\
 &[A] = \begin{bmatrix}
 [G(0,0)+F_1(0,0)+F_2(0,0)] & [G(0,1)+F_1(0,1)+F_2(0,1)] & \dots & [G(0,R)+F_1(0,R)+F_2(0,R)] \\
 [G(1,0)+F_1(1,0)+F_2(1,0)] & [G(1,1)+F_1(1,1)+F_2(1,1)] & \dots & [G(1,R)+F_1(1,R)+F_2(1,R)] \\
 \vdots & \vdots & \ddots & \vdots \\
 [G(R,0)+F_1(R,0)+F_2(R,0)] & [G(R,1)+F_1(R,1)+F_2(R,1)] & \dots & [G(R,R)+F_1(R,R)+F_2(R,R)]
 \end{bmatrix} \\
 &[C]^T = [C_0 \quad C_1 \quad \dots \quad C_R]
 \end{aligned} \right\} \quad (6)$$

In which $[A]$ and $[C]$ are coefficients matrix and unknown vector, respectively. The only unknown parameter in the coefficient matrix $[A]$ is the natural frequency of the tall structure ω . $[C]=0$ is a trivial solution for the resulting system of equations introduced in (6). The natural frequencies are determined through calculation of a non-trivial solution for resulting system of equations. To achieve this, the determinant of the coefficients matrix of the system has to be vanished. Accordingly, a frequency equation in ω is introduced. The roots of the frequency equation are the natural frequencies of tall structure.

3. Novelty of the presented approach

In the previous research papers, various approaches have been presented for calculation of the optimum location of outrigger. For example, minimizing the lateral deflection of the roof or base moment and maximizing the strain energy of the rotational spring. In the presented approach in

this paper, the optimum location of the outrigger is determined by maximization of the first natural frequency of the structure. The location of the outrigger that maximizes the first natural frequency of the structure has been introduced as an optimum location. Maximization of the first natural frequency of the structure maximizes the overall stiffness of the structure. Maximization of the overall stiffness results in minimum lateral deflection in all stories. This new optimization idea is independent of the lateral load pattern.

4. Variations of the first natural frequency with variations of the location of the outrigger

The following parameters are introduced for convenience:

$$\left\{ \begin{array}{l} \alpha = L\sqrt{\frac{AG}{EI}} \\ \beta = L^2\sqrt{\frac{m}{EI}} \\ \bar{K} = \frac{2k_e L}{EI} \\ \xi_{place\ of\ outrigger} = \frac{x_{place\ of\ outrigger}}{L} \end{array} \right. \quad 0 \leq \xi_{place\ of\ outrigger} \leq 1 \quad (7)$$

In which α , β , \bar{K} and $\xi_{place\ of\ outrigger}$ are the parameters corresponding to the stiffness of the structure, mass, stiffness of the outrigger and non-dimensional location of the outrigger, respectively. Parameter α has been changed between 0 to 20. $\alpha=0$ is associated to the structure with only shear behavior and $\alpha=20$ is associated to the structure with only bending behavior. It has been assumed that the structure has two outriggers, one outrigger is assumed that has fixed location at the roof of the structure and location of the second one is assumed that changes along the height of the structure.

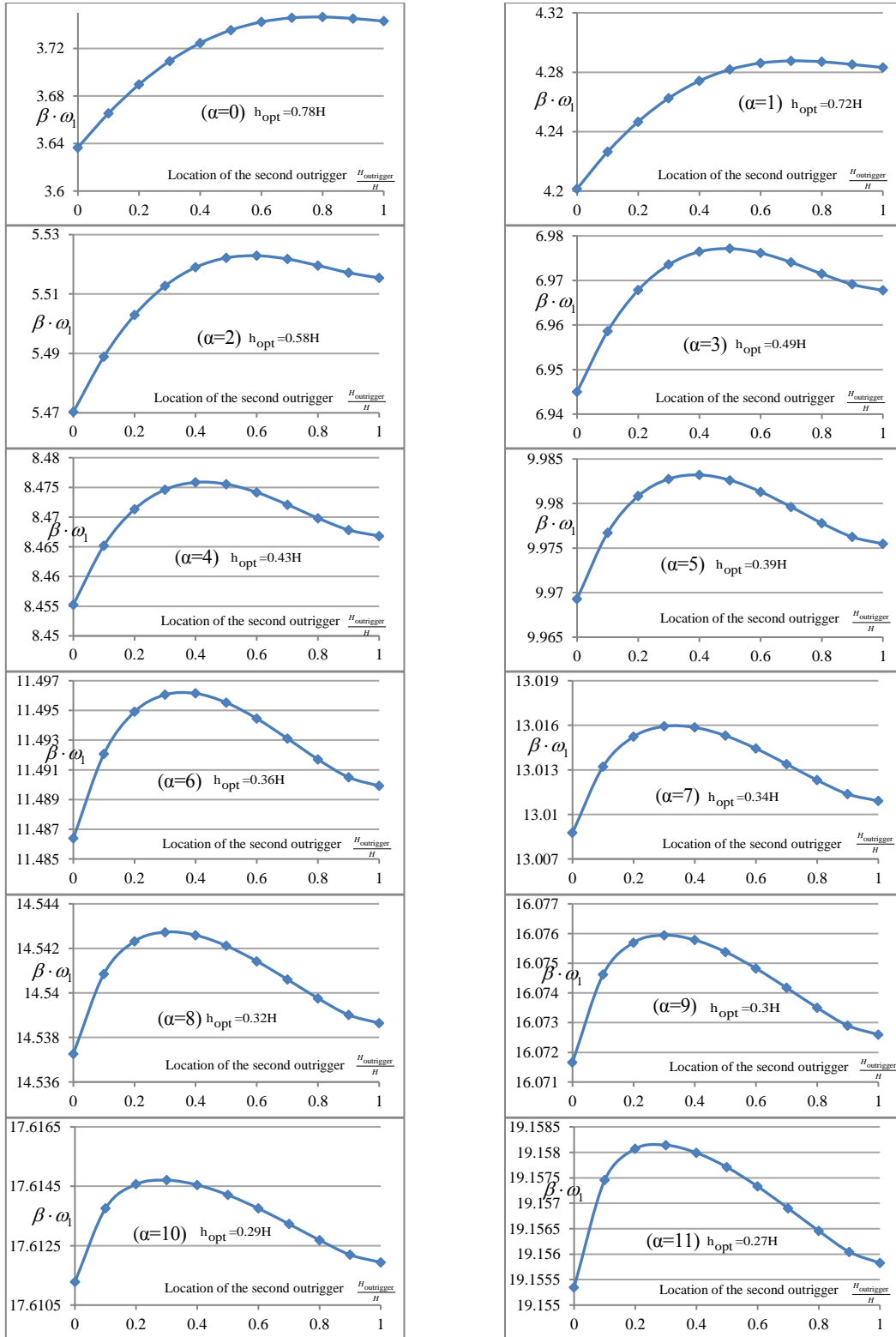
For each value of α ($0 \leq \alpha \leq 20$), the location of the second outrigger has been changed between 0 to H and the first natural frequency of the structure has been calculated.

The variations of the first natural frequency with variations of the location of the second outrigger has been presented in the Fig. 1. The results have been presented for $0 \leq \alpha \leq 20$.

In order to compare the results of Fig. 1, $\alpha=0,6,12$ and 20 has been considered and the corresponding results obtained have been compared in Fig. 2. Boundary value $\alpha=0$ corresponds to the structures with only shear behavior. $\alpha=20$ corresponds to the structures with only bending behavior. While, $4 \leq \alpha \leq 16$ is associated with shear-bending behavior.

5. Optimum location of the outrigger

The peak point of each graph is the location of the outrigger that maximizes the first natural frequency of the structure. Each graph corresponds to a value of α . The peak point presents the optimum location of the outrigger for corresponding value of α . Using presented graphs in the Fig.



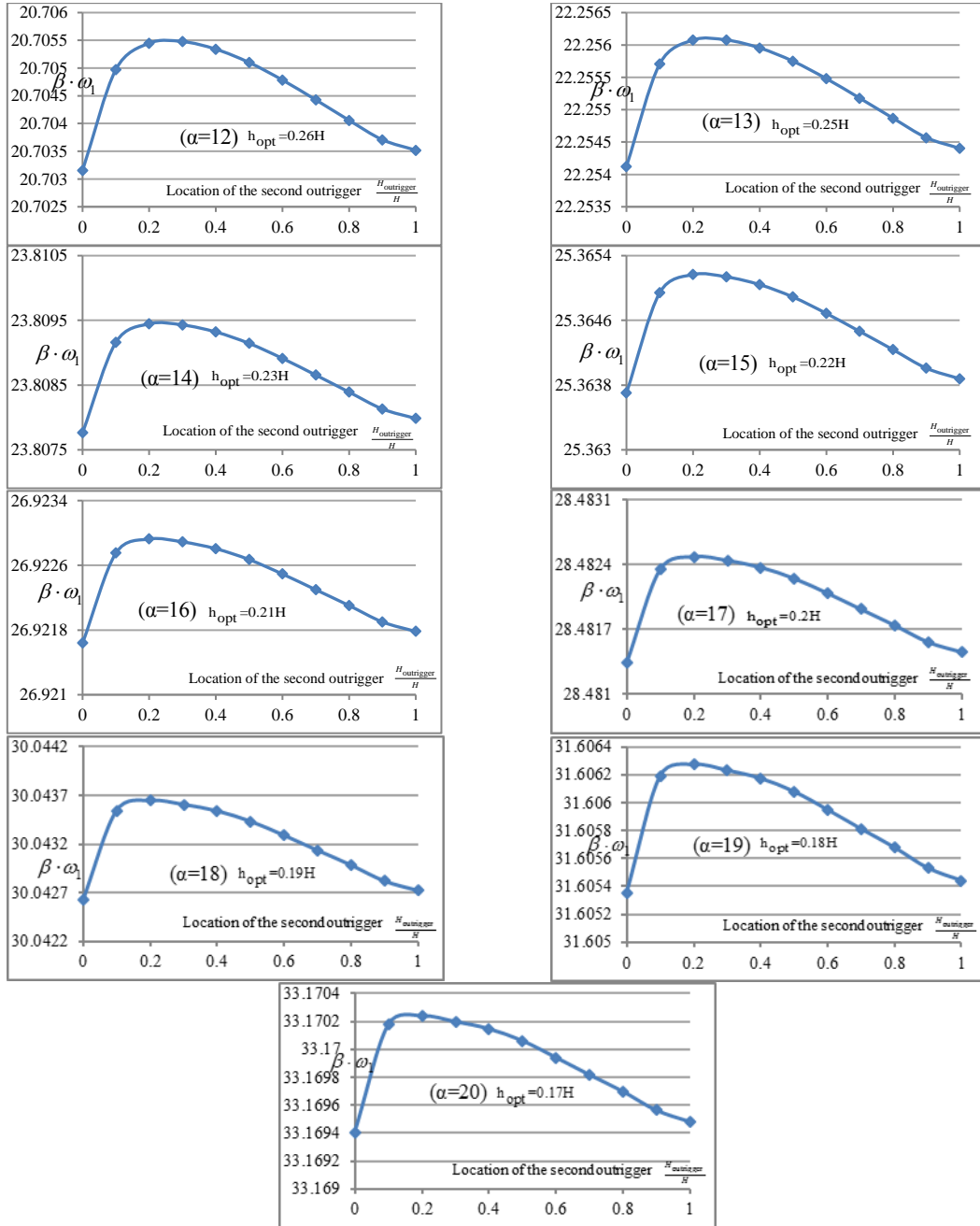


Fig. 1 Variations of the first natural frequency with variations of the location of the second outrigger

1, the optimum location of the outrigger has been calculated for each value of α . The variations of the optimum location of the second outrigger with variations of the parameter α has been presented in the Table 1.

The “fmincon” function of MATLAB program has been used to verify the results of Table 1.

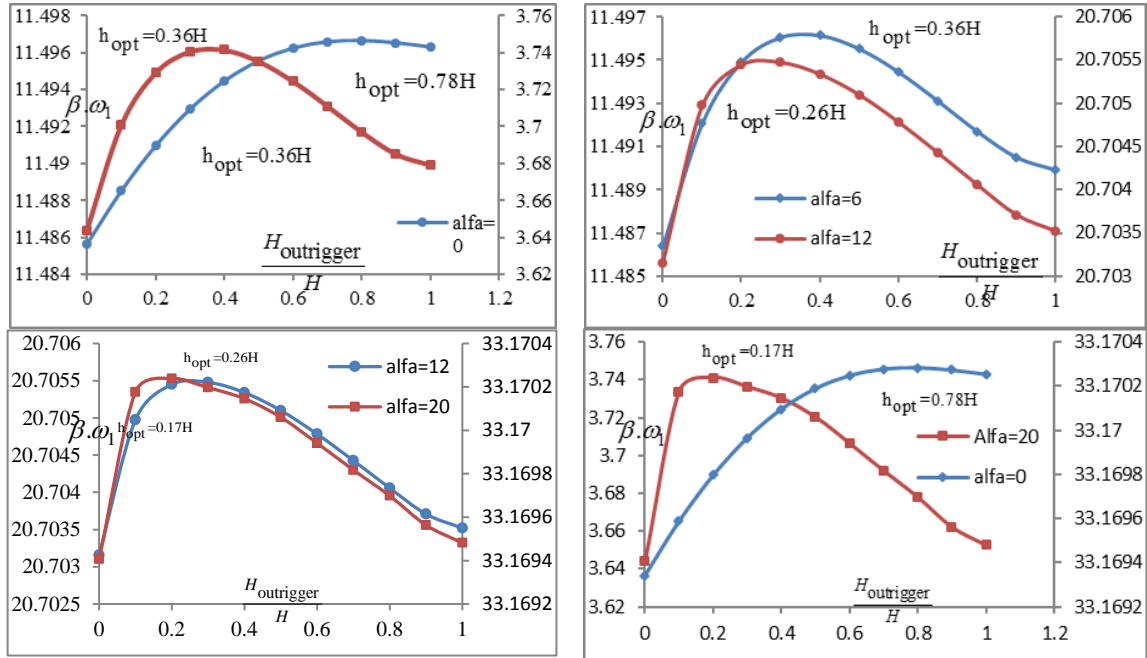


Fig. 2 variation of optimum location for $\alpha=0,6,12,20$

Table 1 The variation of the optimum location of the second outrigger with variation of the α

α	0	1	2	3	4	5	6	7	8	9	10
$\frac{H_{opt}}{H}$	0.78	0.72	0.58	0.49	0.43	0.39	0.36	0.34	0.32	0.3	0.29
α	11	12	13	14	15	16	17	18	19	20	
$\frac{H_{opt}}{H}$	0.27	0.26	0.25	0.23	0.22	0.21	0.2	0.19	0.18	0.17	

“fmincon” attempts to find a constrained minimum of a scalar function of several variables starting at an initial estimate. This is generally referred to as constrained nonlinear optimization or nonlinear programming (MATLAB 7.9.0 R2009b). In this paper the constrained function is “Frequency equation” of the free vibration analysis of the structure based on the location of two outriggers. The matrix of constrain functions of the optimization problem are location of the outriggers which should be between 0 to H and maximization of first natural frequency obtained from frequency equation abovementioned. The results of Table 1 have been presented in the Fig. 3. Boundary value $\alpha=0$ corresponds to the structures with only shear behavior. Also, boundary value $\alpha=20$ corresponds to the structures with only bending behavior. For $0 \leq \alpha \leq 4$ (the structures with only shear behavior), the results of Fig. 3 present the optimum location of the second outrigger approaches to the roof of the structure. While, for $16 \leq \alpha \leq 20$ (the structures with only bending behavior) the optimum location of the second outrigger approaches to the base of the structure. And for $4 \leq \alpha \leq 16$ (the structures with shear-bending behavior) the optimum location of the second outrigger varies between 0.43 H to 0.21 H. H_{opt} is calculated from the base of the structure.

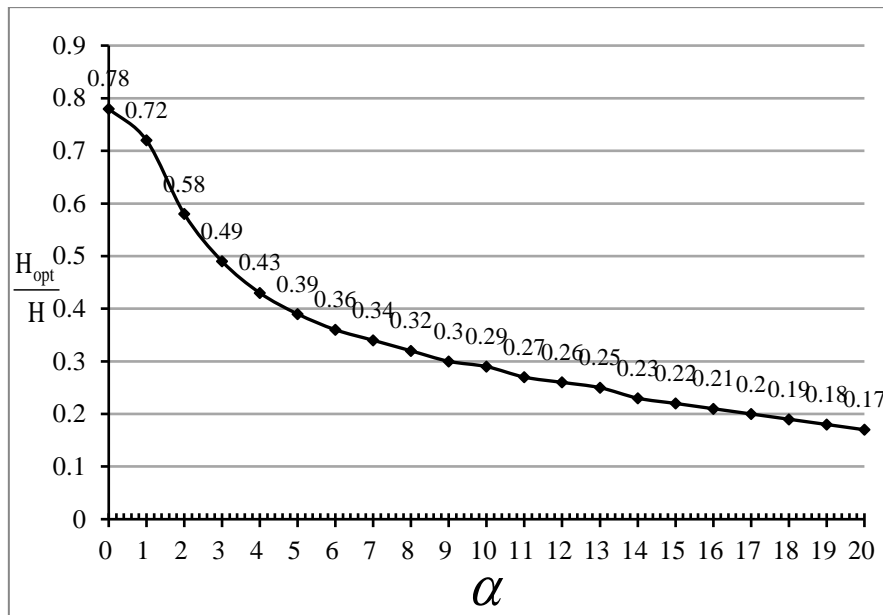


Fig. 3 The variation of the optimum location of the second outrigger with variation of the α

6. Structure behavior with outrigger in the optimum location

In this section, the framed tube combined with shear core, outrigger-belt truss is modelled in the SAP-2000 finite elements software. It is assumed that the first outrigger has a fixed location at the roof of the structure and location of the second outrigger is changed along the height of the structure (Fig. 4).

The structure is analyzed under uniform lateral wind load. The location of the second outrigger is changed along the height of the structure and for each location of the second outrigger, the analysis is carried out. Also, the optimum location of the outrigger which maximizes the first natural frequency of the structure has been determined. The outrigger is located at the optimum location and the analysis is repeated. For each analysis, the lateral deflection of the all stories and the axial force in the columns of the web and flange frames are calculated. Flange frame refers to the perimeter columns that are perpendicular to the lateral load direction and web frame refers to those that are parallel with the lateral load (Fig. 5). The obtained results are compared and a discussion on the results are presented.

6.1 The properties of the modelled structure

A 40-stories tall concrete framed tube combined with shear core and outrigger-belt truss is analyzed using SAP-2000 finite elements software. The structure properties are as follows: story height 3 m, plan dimensions 30 m \times 35 m, the size of the beams, columns and outrigger-belt truss elements 80 cm \times 80 cm, modulus of elasticity $E = 2 \times 10^9$ kg/m², shear modulus of elasticity $G = 8 \times 10^8$ kg/m² poisson's ratio $\nu = 0.25$, the concrete volumetric mass density $\rho = 2400$ kg/m³, the thickness of the roof slab 30 cm, the dimensions of the shear core 5 m \times 5 m, the thickness of the shear core 25 cm, the center-to-center distance of the perimeter columns 2.5 m, the height of the

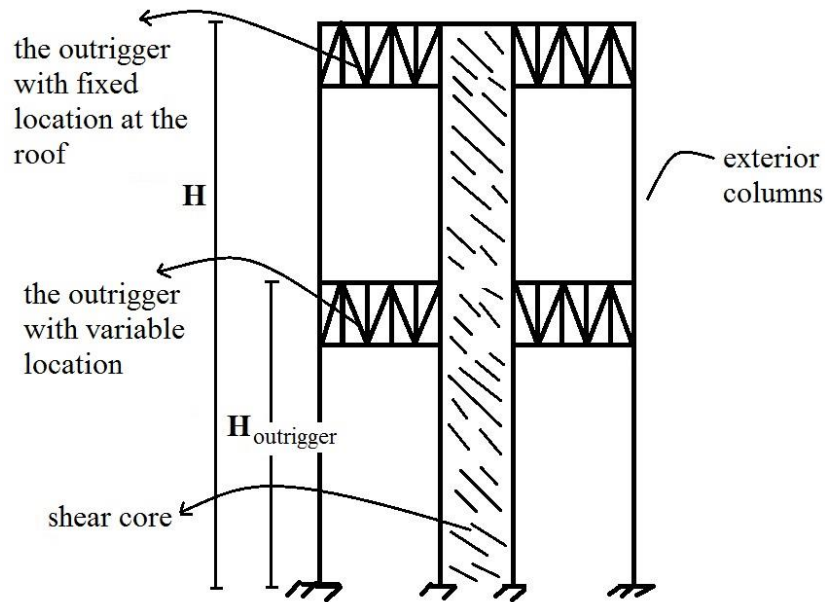


Fig. 4 The structure with a fixed outrigger-belt truss at the top and an outrigger-belt truss with variable location along the height

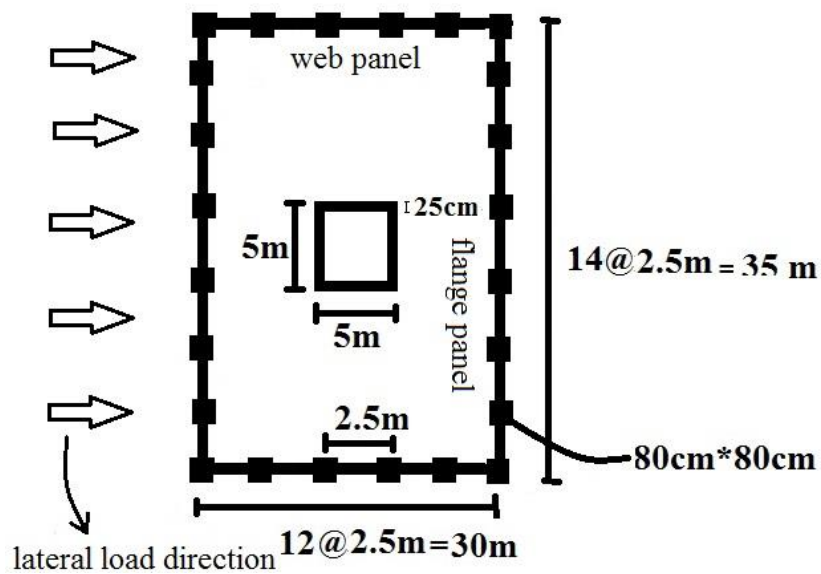


Fig. 5 Plan of the modelled structure and lateral load direction

outrigger-belt truss structure 6 m. The structure has two outrigger-belt trusses. It is assumed that the first outrigger has a fixed location at the roof of the structure and location of the second outrigger is changed along the height of the structure. The properties of the structure have been presented in the Figs. 5 and 6.

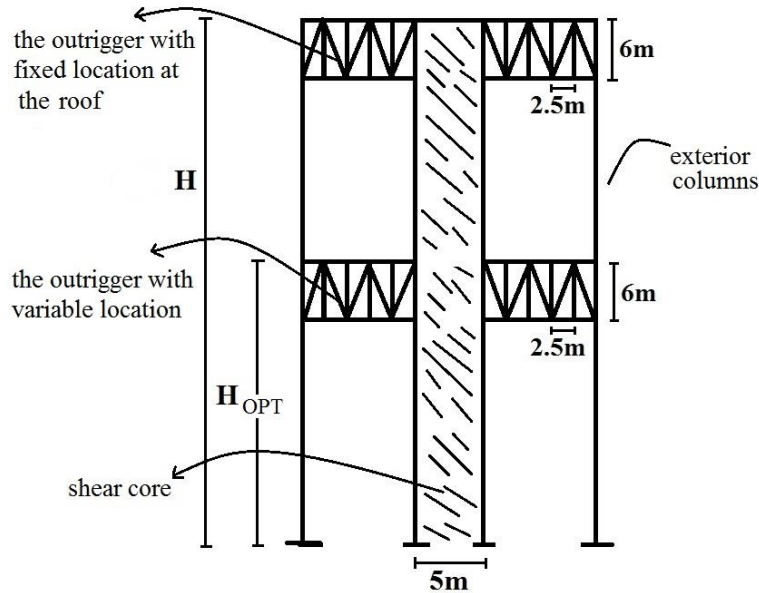


Fig. 6 The properties of the modelled structure

6.2 The analysis results

6.2.1 The optimum location of the outrigger

In the modelling, the first outrigger has a fixed location at the roof of the structure and location of the second outrigger has been changed along the height of the structure. The location of the outrigger which maximizes the first natural frequency of the structure is considered as optimum location. This location has been determined as $H_{opt} = 0.3 H$.

The location of the second outrigger has been changed between $0.1 H$ to $0.9 H$. For each location of the second outrigger, the lateral deflections of the all stories and the axial force in the web and flange columns of the structure have been calculated. Also, the second outrigger has been located at the optimum location $H_{opt} = 0.3 H$ and the mentioned analysis has been repeated.

6.2.2 Lateral deflection of the stories

The lateral deflection of all stories has been presented in the Fig. 7. The continuous line presents the lateral deflection of the stories when the second outrigger has been located at the optimum location. The analysis results present the lateral deflection of the all stories has been minimized when the second outrigger has been located at the optimum location $H_{opt} = 0.3 H$.

6.2.3 Axial force in the columns of the web and flange panels

Ideal cantilevered behavior of the framed tube results in uniformly distributed axial force in the columns of the flange panel and linearly distributed axial force in the columns of the web panel. The shear lag phenomena cause a cubic and parabolic distribution of the axial force in the columns of the web and flange panels, respectively. Various methods have been presented for decrease of the shear lag in the framed tubes. Decrease of the shear lag results in more uniform distribution of the axial force in the columns of the flange panel.

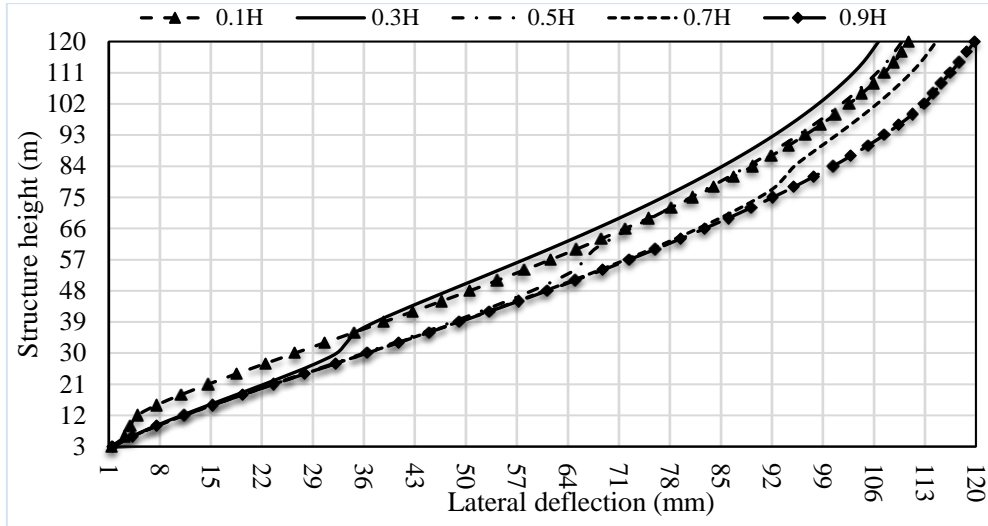


Fig. 7 Lateral deflection of the structure with various locations of the second outrigger

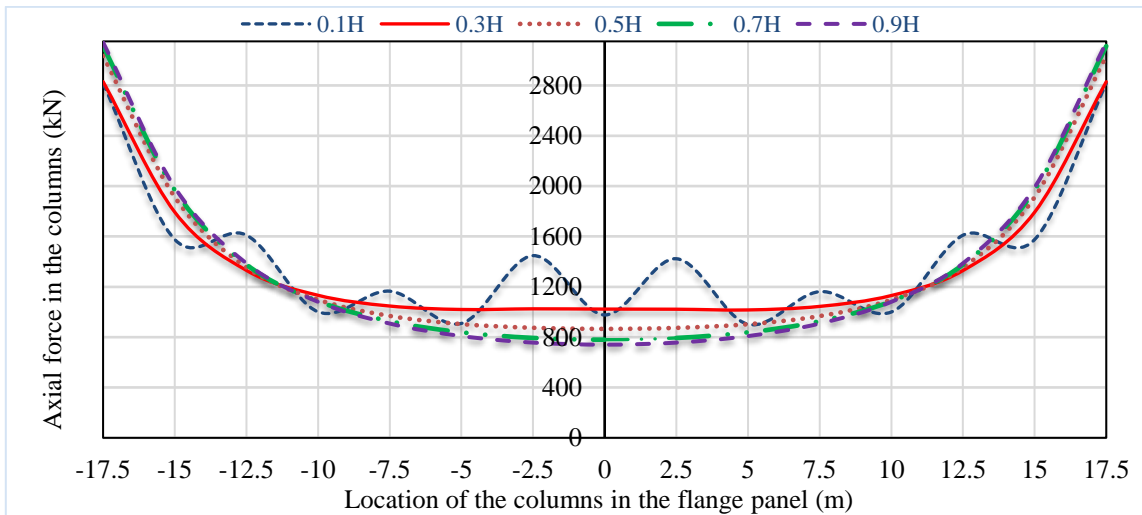
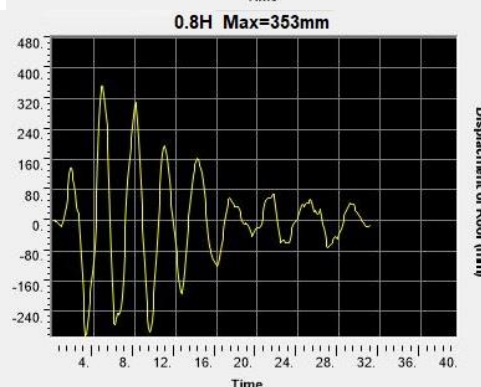
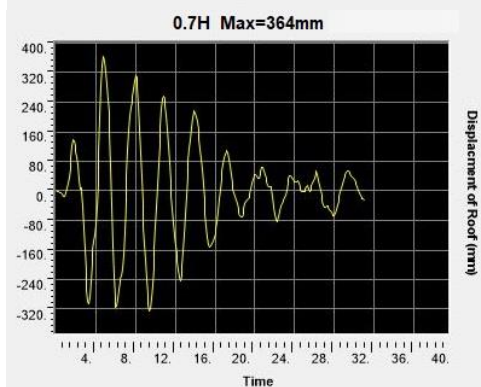
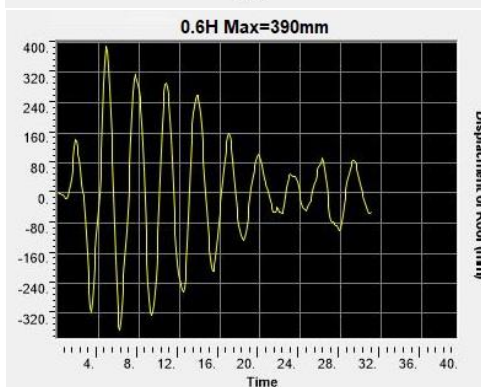
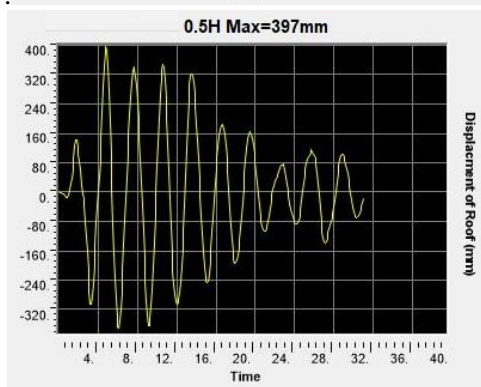
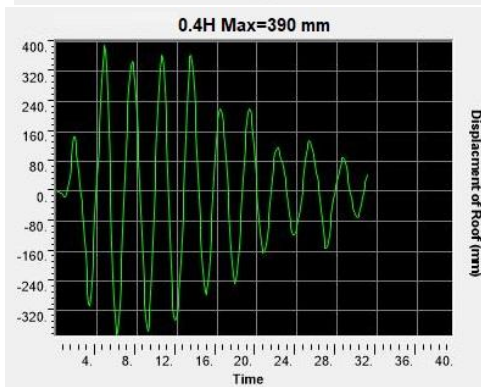
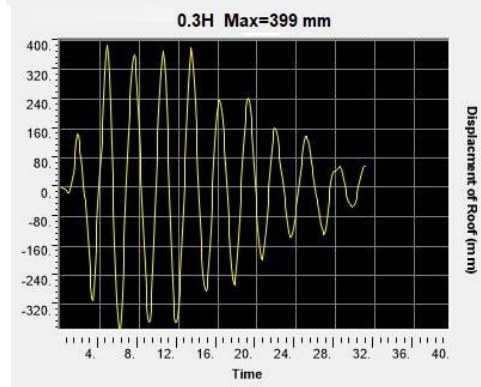
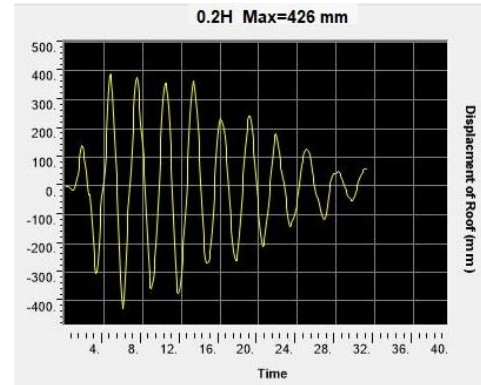
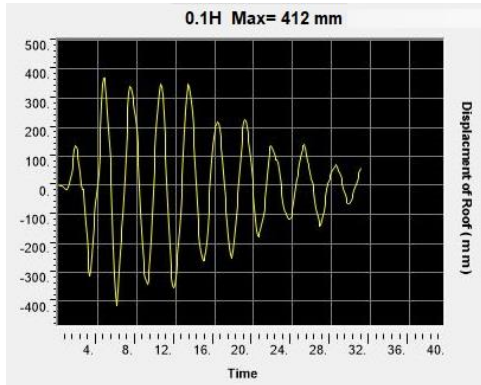


Fig. 8 Axial force in the columns of the flange panel with various locations of the second outrigger

Similar to the previous section, the location of the second outrigger has been changed along the height. For each location, the axial force in the columns of the flange panel has been calculated. Also, the analysis has been repeated when the second outrigger has been located in the optimum location. By changing the location of the second outrigger, the distribution of the axial force in the flange columns changes. Fig. 8 presents the distribution of the axial force in the columns of the flange panel for various locations of the second outrigger.

In the Fig. 8, the continuous red line presents the distribution of the axial force in the columns of the flange panel when the second outrigger has been located at the optimum location. The results of the analysis present when the second outrigger is located in the optimum location, the distribution of the axial force is more uniform. This result proves optimum location of the outrigger can decrease the shear lag phenomena in the framed tube.



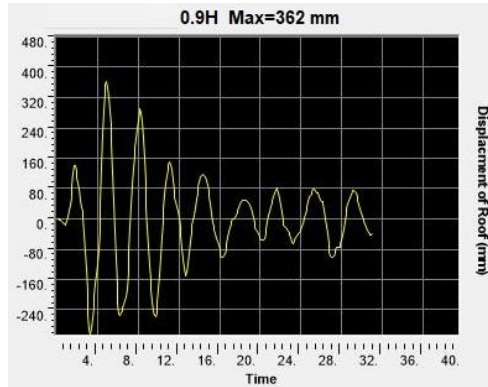


Fig. 9 Lateral displacement of roof under El Centro earthquake

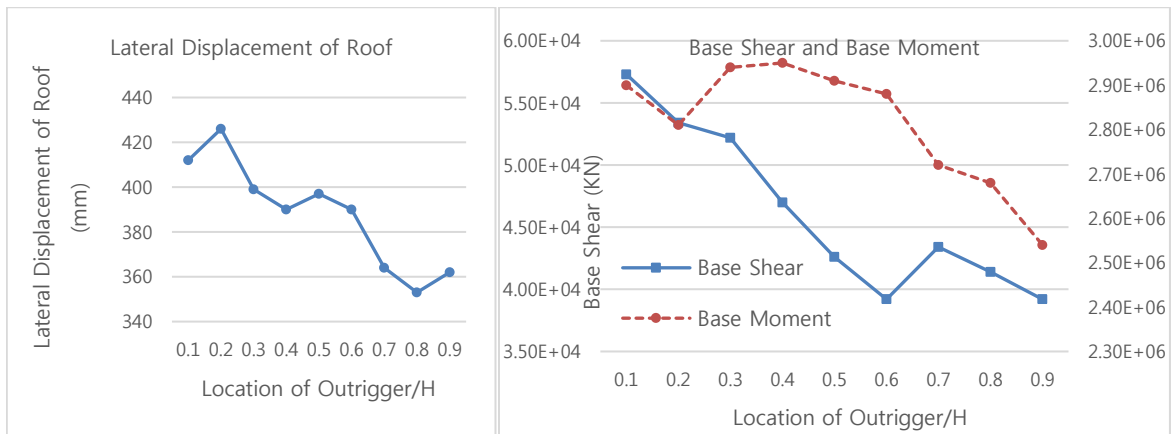


Fig. 10 Variation of lateral displacement of roof, base shear and base moment with location of outrigger under El Centro earthquake

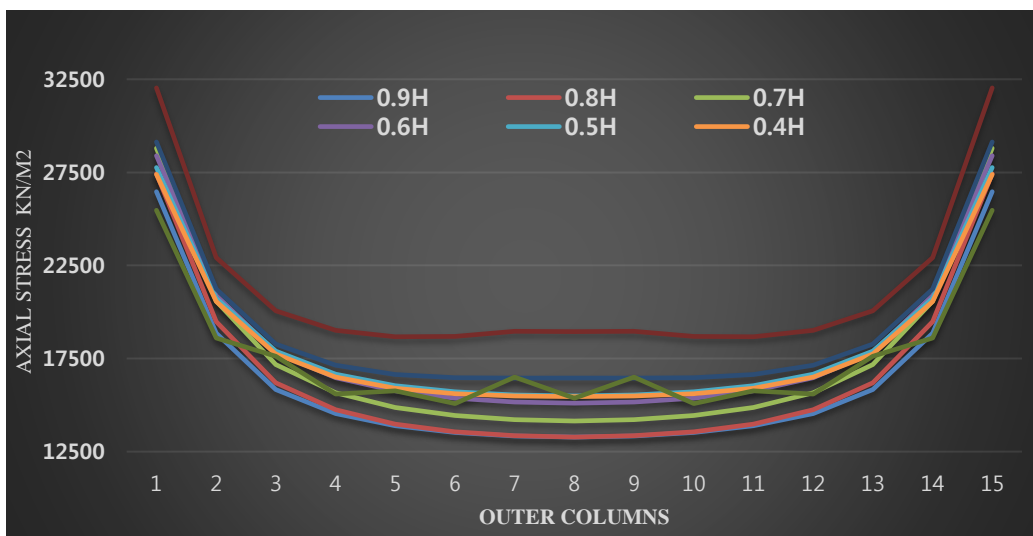


Fig. 11 variation of axial stress in the outer columns with location of outrigger under El Centro earthquake

6.2.4 Time-history analysis

In order to investigate the response of the structure under earthquake, a time-history analysis has been carried out under El Centro earthquake. The lateral displacement of Roof has been calculated and presented in the Fig. 9.

Fig. 10 shows the variation of lateral displacement of roof with location of outrigger. If the minimizing of roof displacement be considered, the optimum location of outrigger is 0.8 H. Also, Fig. 10 presents the variation of Base Moment and Base Shear with location of outrigger. If minimizing the base moment or base shear be considered, the optimum location of outrigger is 0.9 H.

The optimum location of outrigger based on the minimizing the axial stress in the outer columns has been presented in Fig. 11. This result show that the axial stress in the outer columns is minimized when the location of outrigger is 0.8 H.

7. Conclusions

The optimum location of the belt truss-outrigger for a combined system of framed tube, shear core and outrigger-belt truss has been calculated. The optimum location has been determined by maximization of the first natural frequency. The location of the belt truss-outrigger that maximizes the first natural frequency of the structure has been introduced as an optimum location. For structures with only shear behavior, the optimum location of the second outrigger was approached to the roof of the structure. While, for structures with only bending behavior, the optimum location was approached to the base of the structure. And for structures with shear-bending behavior, the optimum location of the second outrigger varied between 0.43 H to 0.21 H. With various locations of the outrigger, the lateral deflection of the all stories and axial force in the columns of the outer tube have been calculated. The analysis was repeated by locating the outrigger-belt truss at the optimum location. The analysis results have been compared and effect of the optimum location on the lateral deflection and the shear lag phenomena have been investigated. The results of the analysis present when the second outrigger is located in the optimum location, the lateral deflection of the all stories are minimized. Also, the optimum location of the outrigger can decrease the shear lag phenomena in the framed tube.

References

- Alavi, A., Rahgozar, P. and Rahgozar, R. (2018), "Minimum-weight design of high-rise structures subjected to flexural vibration at a desired natural frequency", *Struct. Des. Tall Spec.*, **27**(15), e1515. <https://doi.org/10.1002/tal.1515>.
- Akbulut, M., Sarac, A. and Ertas, A.E. (2020), "An investigation of non-linear optimization methods on composite structures under vibration and buckling loads", *Adv Comput. Des.*, **5**(3), 209-231. <http://dx.doi.org/10.12989/acd.2020.5.3.209>.
- Beghini, A., Beghini, L.L., Baker, W.F. and Paulino, G.H. (2014), "Buckling and stiffness optimization of tall buildings", *Struct. Congress 2014*, 2537-2547. <https://doi.org/10.1061/9780784413357.222>.
- Diaz, A.R. and Kikuchi, N. (1992), "Solutions to shape and topology eigenvalue optimization problems using a homogenization method", *Int. J. Numer. Meth. Eng.*, **35**(7), 1487-1502. <https://doi.org/10.1002/nme.1620350707>.
- Niu, F., Xu, S. and Cheng, G. (2011), "A general formulation of structural topology optimization for

- maximizing structural stiffness”, *Struct. Multidiscip. O.* **43**(4), 561-572. <https://doi.org/10.1007/s00158-010-0585-8>.
- Farghaly, A. (2016), “Seismic assessment of slender high-rise buildings with different shear walls configurations”, *J. Adv. Comput. Des.*, **1**(3), 221-234. <http://dx.doi.org/10.12989/acd.2016.1.3.221>.
- Gholipour, M. and Mazloom, M. (2018), “Seismic response analysis of mega-scale buckling-restrained bracing systems in TALL buildings”, *J. Adv. Comput. Des.*, **3**(1), 17-34. <http://dx.doi.org/10.12989/acd.2018.3.1.017>.
- Hoenderkamp, J.C.D. (2008), “Second outrigger at optimum location on high-rise shear wall”, *Struct. Des. Tall Spec.*, **17**(3), 619-634. <https://doi.org/10.1002/tal.369>.
- Hoenderkamp, J.C.D. and Bakker, M.C.M. (2003), “Analysis of high-rise braced frames with outrigger”, *Struct. Des. Tall Spec.*, **12**(4), 335-350. <https://doi.org/10.1002/tal.226>.
- Kamgar, R. and Rahgozar, R. (2017), “Determination of optimum location for flexible outrigger systems in tall buildings with constant cross section consisting of framed tube, shear core, belt truss and outrigger system using energy method”, *Int. J. Steel Struct.*, **17**(1), 1-8. <https://doi.org/10.1007/s13296-014-0172-8>.
- Kamgar, R. and Saadatpour, M. (2012), “A simple mathematical model for free vibration analysis of combined system consisting of framed tube, shear core, belt truss and outrigger system with geometrical discontinuities”, *Appl. Math. Model.*, **36**(10), 4918-4930. <https://doi.org/10.1016/j.apm.2011.12.029>.
- Karimi, M., Kheyroddin, A. and Shariatmadar, H. (2020), “Relationships for prediction of backstay effect in TALL buildings with core-wall system”, *J. Adv. Comput. Des.*, **5**(1), 35-54. <https://doi.org/10.12989/acd.2020.5.1.035>.
- Kaveh, A. and Ilchi Ghazaan, M. (2016), “Truss optimization with dynamic constraints using UECBO”, *J. Adv. Comput. Des.*, **1**(2), 119-138. <http://dx.doi.org/10.12989/acd.2016.1.2.119>.
- Kaviani, P., Rahgozar, R. and Saffari, H. (2008), “Approximate analysis of tall buildings using sandwich beam models with variable cross-section”, *Struct. Des. Tall Spec.*, **17**(2), 401-418. <https://doi.org/10.1002/tal.360>.
- Lee, J., Bang, M. and Kim, J.Y. (2008), “An analytical model for high-rise wall-frame structures with outriggers”, *Struct. Des. Tall Spec.*, **17**(4), 839-851. <https://doi.org/10.1002/tal.406>.
- Lee, D.K., Kim, J.H., Starossek, U. and Shin, S.M. (2012), “Evaluation of structural outrigger belt truss layouts for tall buildings by using topology optimization” *Struct. Eng. Mech.*, **43**(6), 711-724. <http://dx.doi.org/10.12989/sem.2012.43.6.711>.
- Malekinejad, M., Rahgozar, R., Malekinejad, A. and Rahgozar, P. (2016), “A continuous-discrete approach for evaluation of natural frequencies and mode shapes of high-rise buildings”, *Int. J. Adv. Struct. Eng.*, **8**(3), 269-280. <https://doi.org/10.1007/s40091-016-0129-6>.
- Mohammadnejad, M. and Kazemi, H.H. (2018), “A new and simple analytical approach to determining the natural frequencies of framed tube structures”, *J. Struct. Eng. Mech.*, **65**(1), 111-120. <http://dx.doi.org/10.12989/sem.2018.65.1.111>.
- Mohammadnejad, M. and Kazemi, H.H. (2017), “Dynamic response analysis of a combined system of framed tube, shear core and outrigger-belt truss”, *Asian J. Civil Eng.*, **18**(8), 1211-1228.
- Malekinejad, M. and Rahgozar, R. (2013), “An analytical approach to free vibration analysis of multi-outrigger-belt truss-reinforced tall buildings”, *Struct. Des. Tall Spec.*, **22**(4), 382-398. <https://doi.org/10.1002/tal.703>.
- Malekinejad, M. and Rahgozar, R. (2012), “A simple analytic method for computing the natural frequencies and mode shapes of tall buildings”, *J. Appl. Math. Model.*, **36**(8), 3419-3432. <https://doi.org/10.1016/j.apm.2011.10.018>.
- Mortazavi, A. and Toğan, V. (2017), “Triangular units based method for simultaneous optimizations of planar trusses”, *J. Adv. Comput. Des.*, **2**(3), 195-210. <http://dx.doi.org/10.12989/acd.2017.2.3.195>.
- Pedersen, N.L. (2000), “Maximization of eigenvalues using topology optimization”, *Struct. Multidiscip. O.*, **20**(1), 2-11. <https://doi.org/10.1007/s001580050130>.
- Rahgozar, R., Ahmadi, A. and Sharifi, Y. (2010), “A simple mathematical model for approximate analysis of tall buildings”, *J. Appl. Math. Model.*, **34**(9), 2437-51. <https://doi.org/10.1016/j.apm.2009.11.009>.
- Rahgozar, R., Mahmoudzadeh, Z., Malekinejad, M. and Rahgozar, P. (2015), “Dynamic analysis of

- combined system of framed tube and shear walls by galerkin method using B-spline functions”, *Struct. Des. Tall Spec.*, **24**(8), 591-606. <https://doi.org/10.1002/tal.1201>.
- Rahgozar, R., Ahmadi, A.R., Ghelichi, M., Goudarzi, Y., Malekinejad, M. and Rahgozar, P., (2014), “Parametric stress distribution and displacement functions for tall buildings under lateral loads”, *Struct. Des. Tall Spec.*, **23**(1), 22-41. <https://doi.org/10.1002/tal.1016>.
- Tavakoli, R., Kamgar, R. and Rahgozar, R. (2019), “Seismic performance of outrigger-belt truss system considering soil-structure interaction”, *Int. J. Adv. Struct. Eng.*, **11**(1), 45-54. <https://doi.org/10.1007/s40091-019-0215-7>.
- Tavakoli, R., Kamgar, R. and Rahgozar, R. (2018), “The best location of belt truss system in tall buildings using multiple criteria subjected to blast loading”, *Civil Eng.*, **4**(6), 1338-1353. <http://dx.doi.org/10.28991/cej-0309177>
- Tejani, G., Savsani, V.J., Patel, V.K. and Bureerat, S. (2017), “Topology, shape, and size optimization of truss structures using modified teaching-learning based optimization”, *J. Adv. Comput. Des.*, **2**(4), 313-331. <http://dx.doi.org/10.12989/acd.2017.2.4.313>.
- Zhou, Y., Zhang, C. and Lu, X. (2016), “An inter-story drift-based parameter analysis of the optimal location of outriggers in tall buildings”, *Struct. Des. Tall Spec.*, **25**(5), 215-231. <https://doi.org/10.1002/tal.1236>.

WT

